

ON THE MEASUREMENT PRINCIPLES OF SEMICONDUCTOR DOPANT PROFILES

By

A. AMBRÓZY

Department of Electronics Technology, Technical University, Budapest

(Received January 13, 1976)

The dopant profile is one of the main characteristics of the electron devices' microstructure. Its control during as well as at the end of manufacturing yields important information on the final utility of the device in preparation. In some cases, if the doping influences only parameters of minor importance, one may be satisfied with sampled control of dopant profile. However, the figure of merit of tuning varactors depends essentially on that profile: here frequent control is indispensable.

During the development of a profile plotter based on the idea of the author [1] it has become more and more apparent that in the rich and rapidly growing literature of dopant profile measurements there are some contradictions as well as imperfectly defined terms or boundary conditions. The aim of this paper is to summarize the theoretical principles and limitations. Further paper(s) are intended to deal with special varactor topics and the measuring instrument.

In the first part of this paper the non-capacitive methods are briefly outlined. Their majority is destructive, therefore sampling only is advisable.

The second part is more detailed. Described are the theoretical principles of $C-U$ and dC/dU profiling including some refinements and the limiting factors.

1. Non-capacitive profiling methods

1.1 Destructive examination of epitaxially grown layers [2]

It seems the simplest way to polish the wafer's surface step by step and to measure the surface resistivity. This latter is a more or less complicated function of the dopant concentration. Evidently, the resolution is rather poor; each mechanical polishing operation roughens the surface. This roughness should be removed by chemical etching so the minimum step in depth is not less than $1 \dots 3 \mu\text{m}$ [3].

Much more controllable is anodic oxidization, the optical thickness measurement of the oxide layer and its removal by fluoric acid. In this manner the thickness of the epitaxial layer can be reduced in relatively small steps [4].

Quite widespread is the beveled polishing. With a bevel angle of $1 \dots 2$ degrees the dopant profile appears magnified by $30 \dots 60$ on the inclined surface.

Any method is used for removing layer(s) there are many ways to measure the surface resistivity, e.g. that by 2—3—4 point probes. Even the one-point probe [5], [6] and a large-area ohmic contact is sufficient for measuring the spreading resistance which — unfortunately — depends not only on the surface resistivity [7]. The temperature dependence of the surface resistivity may also contain some information: heating the specimen the temperature dependence of mobility can be observed first, then the semiconductor becomes intrinsic [8]. Comparing the obtained curve to published ones the dopant concentration can be deduced.

The breakdown voltage between the bulk semiconductor and a point contact is also characteristic of surface concentration although many disturbing additional effects arise [9].

Two electrochemical methods can be placed among the destructive investigations. The first is well known: the electrochemical potential of the semiconductor depends on the dopant concentration. Etching the sample in an electrolyte, the amount of the material removed can be calculated from the total charge flown through the cell and the surface concentration from the cell voltage.

In a recent procedure [10] an electrolyte is used for Schottky-contact and the capacitance of the junction is measured. The electrolyte continuously etches the surface; so the $C(x)$ curve exhibiting the dopant profile is directly obtained.

1.2 Non-destructive examinations

Their majority needs expensive equipment, high theoretical readiness and lacks the speed necessary to routine measurements. Methods such as infrared absorption, plasma resonance or neutron activation may be enumerated here.

All methods mentioned above suit exclusively to investigate epitaxially grown or diffused layers without contact. For diode structures the information taken from the $C-U$ curves is much more appropriate. A recent method [11], however, uses the breakdown $I(U)$ curve from which the region of profile inaccessible for $C(U)$ examination because of the breakdown can be mapped. It may be important for, say, IMPATT structures. The conclusions drawn from the $I(U)$ curve are neither generalization nor subset of that obtained from $C(U)$ relationship but they complement it.

2. Theoretical bases of C(U) method

2.1 Classical theory

The voltage-dependent capacitance of a rectifying junction was observed first by SCHOTTKY and DEUTSCHMANN in 1929 [12]. Theoretical explanation was given by SCHOTTKY in 1942 [13]. Fig. 1 and Eqs 1 to 3 remind of the simplest theory supposing metal-n semiconductor (SCHOTTKY) junction.

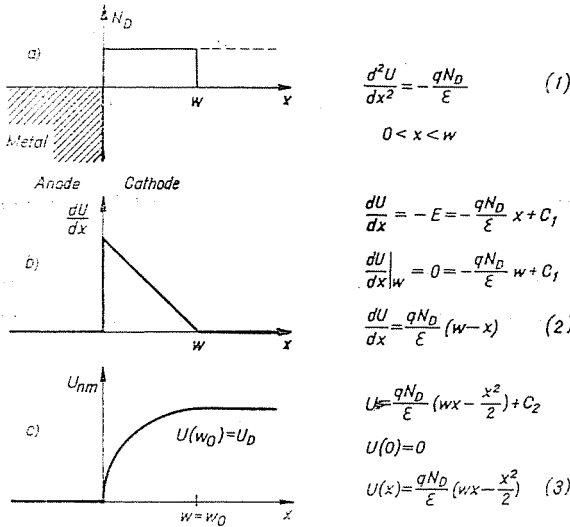


Fig. 1. Space charge (a), electric field (b) and potential (c) in a metal-semiconductor junction

If the potential of the metal side chosen arbitrarily to zero, the n-side is positive everywhere so the built-in potential reversely biases the junction. At zero applied voltage let $x = w_0$ then

$$U(w_0) = \frac{qN_D}{\epsilon} \frac{w_0^2}{2} = U_D \tag{4}$$

An applied voltage U_{AC} between anode and cathode should be added to U_D with the right sign. Since in Fig. 1c a reverse bias corresponds to the upward directed vertical co-ordinate bearing U_{nm} , the right super-position will be $U_D - U_{AC}$. This value remains always positive because an excessive forward bias can be avoided only if $U_{AC} < U_D$. In reverse biased condition $U_D - U_{AC} = U_D + |U_{AC}|$. In this paper throughout this sign convention will be used. Some confusions in the literature originate from careless use of the sign. For brevity, however, instead of U_{AC} we will use U where it is not liable to misunderstanding.

The capacitance of the Schottky-junction can be calculated using Fig. 2 where one constraint is released: the donor concentration may depend on the distance from the junction. Let the total charge be Q in the n -side. If the applied bias changes by $-\delta U_{AC} = -\delta U$, the change in Q will be

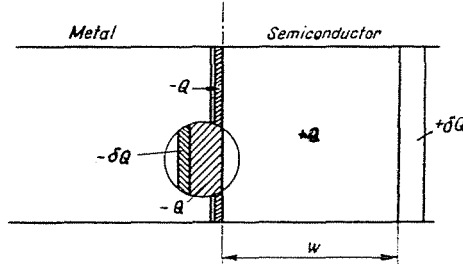


Fig. 2. Enlarged view of the charge balance in a metal-semiconductor junction

$+\delta Q$ because of the change in depletion layer width. Supposing small relative variation of depletion layer width we obtain with good approximation

$$\delta E = -\frac{\delta U}{w} \tag{5}$$

From Gauss' theorem

$$\delta Q = A\epsilon\delta E = -\frac{A\epsilon}{w}\delta U \tag{6}$$

and

$$C = -\frac{\delta Q}{\delta U} = \frac{A\epsilon}{w} \tag{7}$$

2.2 Generalization to arbitrary profiles

Properties of an arbitrary profile are suitably described by an analytical expression from which manifold results can be drawn if necessary. This will be an easily manageable differential equation obtained by the use of Fig. 3 [14].

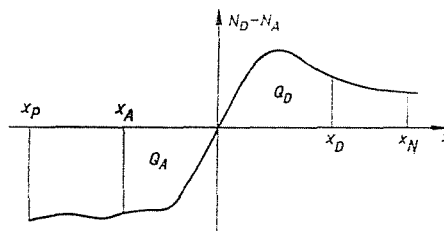


Fig. 3. Arbitrary doping distribution

Let us stipulate that in the region $x_p < x < 0$ only negative, in $0 < x < x_N$ only positive charges (ionized dopants) exist. The boundaries of the depletion layer are X_A and X_D , so

$$w(U) = X_D(U) - X_A(U) \quad (8)$$

and its derivative which will be needed later:

$$\frac{dw}{dU} = \frac{dX_D}{dU} - \frac{dX_A}{dU}. \quad (9)$$

The total charge at the acceptor side is

$$Q_A = -qA \int_{X_A}^0 N_A(x) dx \quad (10)$$

that changes with respect to X_A

$$\frac{dQ_A}{dX_A} = qAN_A(X_A) \quad (11)$$

Similarly, at the donor side

$$Q_D = qA \int_0^{X_D} N_D(x) dx \quad (12)$$

and

$$\frac{dQ_D}{dX_D} = qAN_D(X_D). \quad (13)$$

The charge against voltage derivatives:

$$\frac{dQ_A}{dU} = \frac{dQ_A}{dX_A} \frac{dX_A}{dU} = qAN_A(X_A) \frac{dX_A}{dU} \quad (14)$$

and

$$\frac{dQ_D}{dU} = qAN_D(X_D) \frac{dX_D}{dU}. \quad (15)$$

From Fig. 2 it is obvious that

$$\frac{dQ_A}{dU} = -\frac{dQ_D}{dU}. \quad (16)$$

Combining (9), (14), (15) and (16):

$$\frac{dw}{dU} = \frac{dQ_D}{dU} \frac{1}{qA} \left[\frac{1}{N_D(X_D)} + \frac{1}{N_A(X_A)} \right] \quad (17)$$

Moreover, with a view on definition (7) the wanted differential equation is

$$\frac{dU}{dw} = - \frac{q}{\varepsilon} N(w) w \quad (18)$$

where

$$N(w) = \frac{N_A(X_A) N_D(X_D)}{N_A(X_A) + N_D(X_D)} \quad (19)$$

Important conclusions drawn from Eqs (18) and (19) are that any measurement based on the voltage dependence of the depletion layer width informs only on $N(w)$ rather than on $N_A(X_A)$ and $N_D(X_D)$. For obtaining one-sided profile a priori knowledge of either the profile on the other side or the grade type (e.g. linear) along the junction is needed. Typical kinds are as follows:

1. $N_A \gg N_D$ for all values of w

$$N(w) = \frac{N_D(X_D)}{1 + \frac{N_D(X_D)}{N_A(X_A)}} \approx N_D(X_D) \quad (20)$$

2. $N_D(x) - N_A(x) = ax \quad x_p < x < x_n$

$$N(w) = \frac{a}{4} w \quad (21)$$

3. If $N_A(X_A)$ is known the following general formula can be used [15]:

$$N_D(X_D) = \frac{N_A(X_A)}{1 - \frac{q}{\varepsilon} w(U) \frac{dw}{dU} N_A(X_A)} \quad (22)$$

From the differential equation (18) the basic formula of all dC/dU methods can be derived immediately:

$$\frac{dU}{dw} = \frac{dU}{dC} \frac{dC}{dw} = \frac{dU}{dC} \left(- \frac{\varepsilon A}{w^2} \right) = - \frac{q}{\varepsilon} N(w) w \quad (23)$$

from which

$$N(w) = \frac{A^2}{qw^3} \frac{dU}{dC} = \frac{C^3}{q\varepsilon A^2} \frac{dU}{dC} \quad (24)$$

where (7) was used twice.

2.3 Deviations at low bias

After accumulating a great amount of experiences, beginning with the mid-sixties, the general validity of the Schottky theory has been questioned. Mainly the near-zero bias region was criticized. The developments of the simple theory, however, are ramified not without contradictions. No unified theoretical explanation has been developed to now.

The models investigated suppose abrupt or linearly graded profiles in general. As a starting hypothesis, $1/C^2$ or $1/C^3$ is plotted vs $U_D - U_{AC}$. From the solutions of (18) namely, for abrupt junction:

$$\begin{aligned} dU &= -\frac{q}{\epsilon} N_D w dw; & U &= -\frac{q}{\epsilon} N_D \frac{w^2}{2}; \\ \frac{1}{C^2} &= -\frac{2U}{qN_D \epsilon A^2} = \frac{2(U_D - U_{AC})}{qN_D \epsilon A^2} \end{aligned} \quad (25)$$

and for linearly graded junction:

$$\begin{aligned} dU &= -\frac{q}{\epsilon} \frac{a}{4} w^2 dw; & U &= -\frac{q}{\epsilon} \frac{a}{12} w^3; \\ \frac{1}{C^3} &= \frac{12(U_D - U_{AC})}{qa\epsilon^2 A^3}. \end{aligned} \quad (26)$$

$1/C^2$ or $1/C^3$ is a linear function of U_{AC} so the hypothesis of abrupt or linear profile may easily be verified or discarded examining the slope. According to (25) and (26), the line intersects the horizontal axis at U_D (Fig. 4). Unfor-

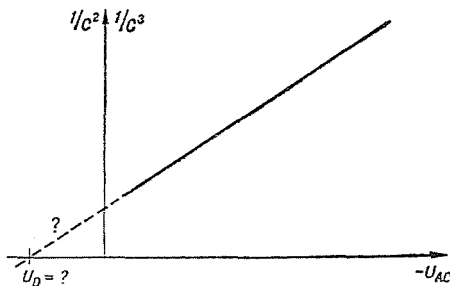


Fig. 4. C^{-2} , C^{-3} vs voltage curves for an abrupt and linearly graded junction, respectively

tunately, this point lies in the forward region, therefore the space charge capacitance alone cannot be measured, and the constant slope line cannot be interpreted. In spite of this, it was believed previously that the intersect

of the extrapolated line gives exactly U_D which can be calculated also in another way.

Using a small signal field theory model, CHANG [16] pointed out that for $U_D - U_{AC} > 1$ V the Schottky solution applied to the abrupt junction was quite true but the extrapolated line intersected at least by $2 kT/q \approx 50$ mV lower than U_D . This correction part depends on the doping rate of the opposite sides of the junction and on the applied bias, Fig. 5 a, e.g. the $1/C^2$ curve shifts parallel with itself if the bias changes.

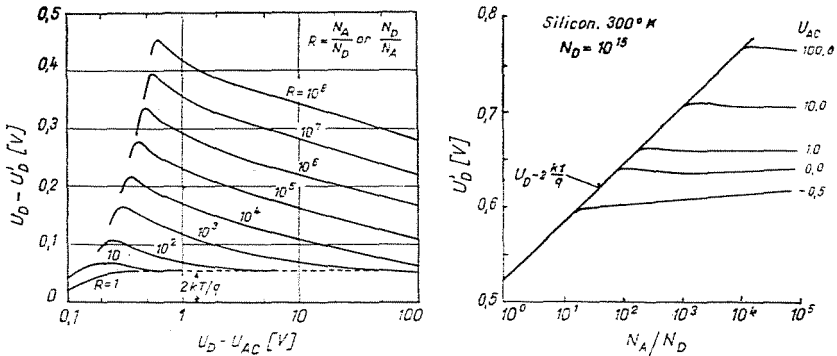


Fig. 5. Corrections for U_D according to [16] (a) and [17] (b)

Almost simultaneously, GUMMEL and SCHARFETTER [17] showed that in a strongly asymmetrical junction the majority carrier tail extending over from the highly doped side caused a considerable deviation of the classic curve, especially at low bias. They worked out a rather complicated potential model for the necessary correction; the results are presented in Fig. 5 b. According to this, at low dopant ratios the Chang's correction of $U_D - 2U_T$ is applicable. For higher asymmetries, however, increasing the applied reverse bias the intersect becomes constant sooner or later and does not follow the theoretical $U_D = U_T \ln N_A N_D / n_i^2$.

The strongly asymmetrical junction aroused other's interest, too. Two subsequent papers by KENNEDY and others [18], [19], starting from numerical solutions of transport and continuity equations proved the dC/dU method to give the majority concentration, $n(x)$ instead of $N(x)$. One of their conclusions is that if the lower doping density in the vicinity of the junction is less than $10^{16}/\text{cm}^3$ the result may be significantly erroneous.

The second paper [19], however, gives a correction equation as follows:

$$N(x) = n(x) + U_T \frac{\varepsilon}{q} \frac{d}{dx} \left[\frac{1}{n(x)} \frac{dn(x)}{dx} \right]. \quad (27)$$

Later on, CARTER, GUMMEL and CHAWLA [20] using likewise a numerical model demonstrated that the equation above was not exactly correct: if the same imagined semiconductor bulk was examined twice so that the Schottky and ohmic contacts were interchanged before the second run, the results based on Eq. (27) were not quite equal.

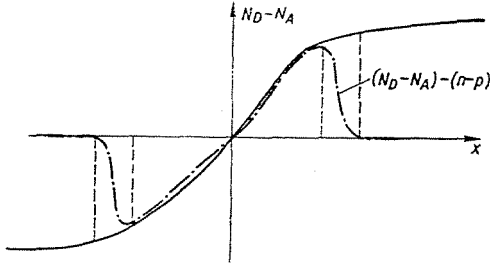


Fig. 6. "Smeared" boundaries of the depleted regions

Until now the "smearedness" of the carrier density in the vicinity of the metallurgical junction has been discussed. Similarly important is the investigation of the depletion layer's boundaries. Earlier calculations supposed abrupt space charge approximation (ASCE). Not abruptly sloping boundaries cause always deviations when the width of sloping region is commensurable with the total dimension of the depletion layer. One such case can be observed at low absolute values of the applied bias (Fig. 6).

KUZMICZ and SWIR [21] checking the validity of the approximation concluded that supposing not too asymmetrical profile the $U_D - 2 U_T$ intersect was acceptable. The solution of the differential equation (18) with the above assumption yields

$$U_{AC} = -\frac{q}{\epsilon} \int_{X_A}^{X_D} xN(x)dx - U_T \left[\ln \frac{N_A(X_A) N_D(X_D)}{n_i^2} - 2 \right] \quad (28)$$

where X_A and X_D are so far unknown. But the integral equation

$$-\int_{X_A}^0 N_A(x) dx + \int_0^{X_D} N_D(x) dx = 0 \quad (29)$$

should also exist. The two unknowns may be calculated from (28) and (29) and with them the corrected capacitance appears as

$$\frac{1}{C} = \frac{X_D - X_A}{\epsilon A} - \frac{kT}{q^2 A} \left[\frac{1}{N_D^2(X_D)} \frac{dN_D(X_D)}{dX_D} - \frac{1}{N_A^2(X_A)} \frac{dN_A(X_A)}{dX_A} \right]. \quad (30)$$

For abrupt junction Eq. (30) gives the classical result: both derivatives in the brackets are zero. For linearly graded junctions using (21):

$$\frac{1}{C} = \frac{w}{\varepsilon A} - \frac{8kT}{Aaq^2} w^{-2} \quad (31)$$

and

$$U_{AC} = -\frac{qa}{12} w^3 - \frac{2kT}{q} \left[\ln \left(\frac{aw}{2n_i} \right) - 1 \right] \quad (32)$$

where $w = X_D - X_A$. The second term of (32) is by $14 kT/3q$ lower than the calculated value of the built-in potential; now this is the corrected value of the intersect.

Only one recent paper [22] gives results not only for the intersect but also for the deviation between the real and classical $C-U$ characteristics. Complicated calculations based on the field theory and involving an intricate equation resulted in a simplified solution:

$$C \approx A \left[\frac{q\varepsilon N_D}{(1 + e^{2\psi})(U_D - U_{AC})} \right]^{1/2} \quad (33)$$

where

$$U_D = \frac{kT}{q} \left[\ln \frac{N_A N_D}{n_i^2} - 2 - \ln \frac{N_A}{N_D} - 2\psi \right]. \quad (34)$$

The first three terms of Eq. (34) resemble to GUMMEL and SCHARFETTER's result; the fourth is represented graphically in Fig. 7. The dashed curves in Fig. 8 correspond to Eq. 33 while the continuous ones are calculated from a more precise but very complicated formula. The numbers along the vertical axis are multiplication factors normalized to the Schottky equation.

2.4 Deviations in narrow structures

In regions where the dopant profile changes abruptly, the majority carrier distribution differs substantially from the doping distribution as it was pointed out by KENNEDY et al. [18], [19]. This difference is due to the existence of a dipole layer which is found near the region of the abrupt change in doping concentrations. Its occurrence can be traced back to the fact that the electrostatic potential inside the doped wafer must be smooth and continuous and therefore cannot follow the abrupt changes in doping concentrations. Such abrupt changes are created by ion implantation [23]. An ion-implanted impurity atom distribution is typically a narrow Gaussian distribution with the center of the Gaussian less than $1 \mu\text{m}$ from the surface with typically only $0,1 \mu\text{m}$ half-width. Under such conditions the ASCE approximation may be misleading.

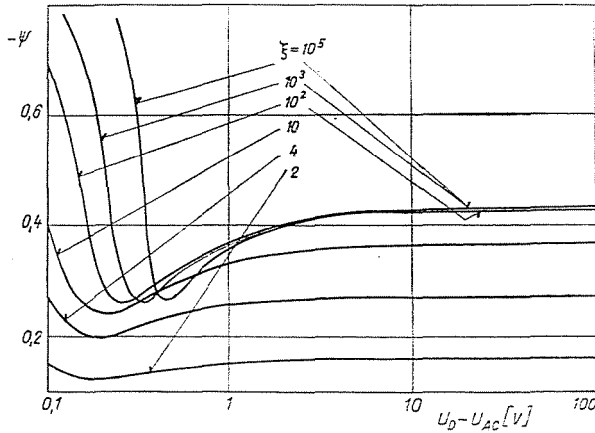


Fig. 7. Correction voltage for U_D [22]

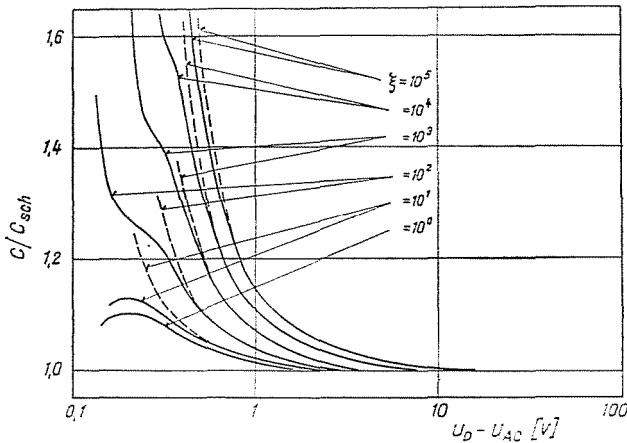


Fig. 8. Normalized capacitance curves at low bias. Dashed lines correspond to (33), for full lines see [22]

The ultimate resolution of the $C-U$ method depends on the so-called extrinsic Debye-length:

$$\lambda = \sqrt{\frac{kT\epsilon}{q^2N}} \tag{35}$$

of the order of $0.1 \mu\text{m}$. $C-U$ data are insensitive to changes in the doping profile within a distance smaller than the Debye length corresponding to the doping on the high side. Profiles determined by this method are expected to show a spatial resolution only of the order of a Debye length [24].

2.5 Possible errors for high reverse bias

Increasing the reverse bias, the intrinsic capacitance of the junction decreases and the relative weight of stray capacitances grows. Their estimation is very difficult: not only the — generally known — mutual capacitance of the measuring instrument but the stray capacitance of the diode itself should be taken into account.

The capacitance of a *Schottky* diode (including the part at the perimeter) is estimated by Copeland [25] as:

$$C = C_0 \left(1 + b \frac{w}{r} \right); \quad b \approx 1,5 \quad (36)$$

where $C_0 = \varepsilon A/w$ and r is the radius of the circular Schottky-contact. For $w/r \ll 1$, as a first approximation,

$$\frac{dC}{dU} \approx \frac{dC_0}{dU} \quad (37)$$

so the derivative of the $C-U$ curve can be measured quite exactly. However, to obtain $N(w)$, according to Eq. (24) C^3 also

$$C^3 = C_0^3 \left(1 + b \frac{w}{r} \right)^3 \approx C_0^3 \left(1 + 3b \frac{w}{r} \right) \quad (38)$$

is needed, which may be considerably erroneous. To obtain $N(x)$ at an acceptable precision, the small area deeply depleted diodes should be avoided, namely because of the small capacitance their measurement is more difficult anyway.

To separate the stray capacitances, SZENTPÁLI [26] proposes an ingenious but intricate solution. Rearranging Eq. 24:

$$\frac{dC}{dU} = \frac{1}{q\varepsilon A^2 N(x)} C^3 \quad (39)$$

and the second derivative

$$\frac{d^2C}{dU^2} = \frac{3C^2}{q\varepsilon A^2 N(x)} \frac{dC}{dU} + \frac{C}{qAN^2(x)} \frac{dN(x)}{dx} \frac{dC}{dU} \quad (40)$$

For $dN/dx = 0$ the second term vanishes. Combining (39) and (40):

$$C = 3 \left(\frac{dC}{dU} \right)^2 \left(\frac{d^2C}{dU^2} \right)^{-1} \quad (41)$$

i.e. the capacitance of the depletion layer can be calculated from the *derivatives* alone. So the stray capacitance C_s is the difference between capacitances C_m (measured) and C calculated from (41)):

$$C_s = C_m - C. \quad (42)$$

It is rather difficult to get the second derivative with sufficient accuracy; furthermore for hyperabrupt structures $dN/dx \neq 0$ and it is *a priori* unknown. Therefore the above described method of obtaining the stray capacitance needs very careful measurements and a lot of calculations which of course can be computerized.

Finally the effect of the conductance parallel to the capacitance to be measured should be mentioned. Increasing the reverse bias the reverse current rises first slowly, then, near the breakdown, sharply. The result of measurement is acceptable if

$$g = \frac{dI_R}{dU_R} \leq \omega C_{\min} D_{\max} \quad (43)$$

where D_{\max} is the maximal loss factor tolerated by the measuring equipment, ω is the angular frequency and C_{\min} is the minimal capacitance to be measured at the highest reverse bias. If for example $D_{\max} = 10^{-2}$, $\omega = 2\pi 10^6$ rad/s and $C_{\min} = 1$ pF the maximum of the parallel conductance is

$$g = 2\pi 10^{-8} \text{ S},$$

a rather severe condition.

The reverse current of the diode consists of two parts. The surface component is proportional to the perimeter of the diode and it increases generally with increasing bias, consequently it corresponds to a constant conductance as a first approximation. The volume component is linearly proportional to the volume of the depletion layer, therefore

$$g_V = \frac{dI_V}{dU} = \frac{dI_V}{dV} \frac{dV}{dU} = \gamma A \frac{dw}{dU} \quad (44)$$

where V is the subscript for volume. Expressing dw/dU by means of Eq. (18)

$$g_V = -\gamma A \frac{\varepsilon}{q} \frac{1}{N(w)w} = -\frac{\gamma C}{qN(w)}, \quad (45)$$

a positive term since $\gamma < 0$. Introducing the "volume" loss factor

$$D_V = \frac{g_V}{\omega C} = -\frac{\gamma}{\omega q N(w)} \quad (46)$$

and the "surface" factor

$$D_S = \frac{g_S}{\omega C(U)} \quad (47)$$

the sum of both must not exceed D_{\max} :

$$D_{\max} \leq D_V + D_S = -\frac{\gamma}{\omega q N(w)} + \frac{g_S}{\omega C(U)}. \quad (48)$$

Since the first term depends only on the doping profile rather than on the area of the diode, it is advisable to decrease the second term by increasing the area of the diode. C is linearly proportional to the area while g_S increases slower: the perimeter is proportional to the square root of the area.

3. Conclusion

Dopant profiling by the use of $C-U$ or dC/dU method raises the question of the validity of depletion theory. At the low and the high ends of the bias curve as well as for narrow structures there are considerable deviations from the classical Schottky theory.

Summary

The dopant profile is one of the main characteristics of the electron device's microstructure. During the development of a profile plotter based on an earlier idea of the author some contradictions became apparent in the developments of the simple depletion theory. At the low and the high ends of the bias curve as well as for narrow structures there are considerable deviations from the classical Schottky theory. Further papers will describe the developed measuring instrument for which theoretical principles and limitations have been summarized.

References

1. AMBRÓZY, A.: A simple dC/dV measurement method and its application. *Sol. St. El.* **13**, 1970/3, pp. 347–353.
2. FRANK, H.: Některé problémy měření epitaxních a difundovaných vrstev polovodivců. *Ces. Casopis pro Fysiku*, A **23**, 1973, pp. 253–271.
3. FULLER, C. S.—DITZENBERGER, J. A.: Diffusion of donor and acceptor elements in silicon. *J. Appl. Phys.* **27**, 1956/5, pp. 544–553.
4. TSAI, J. C. C.: Shallow phosphorus diffusion profiles in silicon. *Proc. IEEE* **57**, 1969/9, pp. 1499–1506.
5. MAZUR, R. G.—DICKEY, D. H.: A spreading resistance technique for resistivity measurements on Si. *J. El. Chem. Soc.* **113**, 1966/3, pp. 255–259.
6. FRANK, H.—ABDEL AZIM, S.: Measurement of diffusion profile of Zn in n-type GaAs by a spreading resistance technique. *Sol. St. El.* **10**, 1967/7, pp. 727–728.

7. SCHUMANN, P. A.—GARDNER, E. E.: Application of multilayer potential distribution to spreading resistance correction factors. *J. El. Chem. Soc.* **116**, 1969/1, pp. 87—91.
8. SHIVE, J. N.: *The Properties, Physics and Design of Semiconductor Devices*. D. Van Nostrand, Princeton, N. J. 1960.
9. GARDNER, E. E. & AL.: Comparison of resistivity measurement techniques on epitaxial Silicon. *SSE* **6**, 1963/3, pp. 311—313.
10. AMBRIDGE, T.—FAKTOR, M. M.: Electrochemical technique for plotting of donor concentration over large depths. *Electronics Letters* **10**, 1974/10, pp. 202—205.
11. GLOVER, G. H.—TANTRAPORN, W.: Doping profile measurements from avalanche space charge resistance. *J. App. Phys.* **46**, 1975/2, pp. 867—874.
12. SCHOTTKY, W.—DEUTSCHMANN, W.: Zum Mechanismus der Richtwirkung in Kupferoxydulgleichrichtern. *Phys. Z.* **30**, 1929, pp. 839—846.
13. SCHOTTKY, W.: Vereinfachte und erweiterte Theorie der Randschicht-Gleichrichter. *Z. Phys.* **118**, 1942, pp. 539—592.
14. OPDORP, C.: Evaluation of doping profiles from capacitance measurements. *Sol. St. El.* **11**, 1968, pp. 397—406.
15. DE MAN, H. J. J.: On the calculation of doping profiles from C(V) measurements on two-sided junctions. *IEEE Tr.* **ED—17**, 1970/12, pp. 1087—1088.
16. CHANG, Y. F.: The capacitance of pn junctions. *Sol. St. El.* **10**, 1967, pp. 281—287.
17. GUMMEL, H. K.—SCHARFETTER, D. L.: Depletion layer capacitance of p+n step junctions. *J. Appl. Phys.* **38**, 1967/5, pp. 2148—2153.
18. KENNEDY, D. P. & AL.: On the measurement of impurity atom distributions in silicon by the differential capacitance technique *IBM J. Res. Develop.* **12**, 1968, pp. 399—409.
19. KENNEDY, D. P.—O'BRIEN, R. R.: On the measurement of impurity atom distributions by the differential capacitance technique. *IBM J. Res. Develop.* **13**, 1969, pp. 212—214.
20. CARTER, W. E. & AL.: Interpretation of capacitance vs. voltage measurements of pn-junctions. *Sol. St. El.* **15**, 1972, pp. 195—201.
21. KUZMICZ, W.—SWIT, A.: The built-in voltage and space charge layer capacitance of PN-junctions. *Sol. St. El.* **17**, 1974, pp. 457—463.
22. DJURIC, Z. & AL.: P—N transition capacitance. *Sol. St. El.* **14**, 1971, pp. 457—466.
23. WU, C. P. & AL.: Limitations of the CV technique for ion-implanted profiles. *IEEE Tr.* **ED—22**, 1975/6, pp. 319—329.
24. JOHNSON, W. C.—PANOUSIS, P. T.: The influence of the Debye length on the C—V measurement of doping profiles. *IEEE Tr.* **ED—18**, 1971/10, pp. 965—973.
25. COPELAND, J. A.: Diode edge effect on doping profile measurements. *IEEE Tr.* **ED—17**, 1970/5, pp. 404—407.
26. SZENTPÁLI, B.: A direct method for measuring the stray capacitance of diodes. *Int. J. Electronics* **38**, 1975/2, pp. 259—263.

Prof. Dr. András AMBRÓZY, H-1521 Budapest